POLITECNICO DI TORINO
Repository ISTITUZIONALE

On the Heat Transfer in Particle-laden Turbulent Flows: the Effect of Collision in an Anisothermal Regime

(Article begins on next page)

29 April 2024

On the Heat Transfer in Particle-laden Turbulent Flows: the Effect of Collision in an Anisothermal Regime

Hamid Reza Zandi Pour[1], Michele Iovieno[1]
[1] Dipartimento di Ingegneria Meccanica e Aerospaziale, Politecnico di Torino
Corso Duca degli Abruzzi 24, 10129 Torino, Italy
hamid.zandipour@polito.it; michele.iovieno@polito.it

Abstract – In this study, we investigate a two-way thermally coupled collisional turbulent particle-laden flow using Eulerian-Lagrangian point-particle direct numerical simulations. Our aim is to examine the impact of inter-particle collisions on heat transfer in a time-evolving thermal mixing layer that develops between two homothermal regions, which are carried by a homogeneous and isotropic turbulent flow. Our results cover Stokes numbers between 0.2 and 3, with a ratio of thermal Stokes number to Stokes number equal to 4.43, at a Taylor microscale Reynolds number up to 124. We found that particle collisions tend to reduce the particle temperature-velocity correlation, which results in a small decrease in the average heat transfer compared to a collisionless regime at large Stokes numbers.

Keywords: heat transfer, particle-laden flow, turbulent mixing, inter-particle collisions

1. Introduction

Particle-laden turbulent flows are omnipresent in nature and industry. Archetypal examples are dispersed liquid fuel droplets in combustors, catalytic particles in process technology, suspended pollutants, water droplets, powder-snow avalanches and volcanic ashes in atmosphere, and plankton species and plastic particles in oceans and sediments in rivers. Therefore, the dynamics of inertial particles suspended in a turbulent flow has been an active area of research in many scientific disciplines and it has been under experimental and computational investigation for decades. On the other hand, particle-particle collisions play a significant role in many phenomena even in relatively diluted suspensions. For instance, collisions between water droplets in clouds are a necessary condition for precipitation formation from cloud droplets and ice crystals, while, particle-particle collisions have a profound impact on the onset and evolution of sandstorms [1]. In these processes, the background turbulence of the carrier flow favors inter-particle collisions. The mechanisms of the collision rate enhancement by background turbulence have only become clear in the past few years, and the underlying physics is currently qualitatively well understood, although quantifying collision rates of small particles suspended in turbulent flow fields may require more advancement.

Despite the numerous experimental works which have been done on single-phase turbulent flows, very little experimental investigations exist concerning particle-laden flow and collisions of suspended particles, primarily due to the difficulties in Lagrangian measurements. The problem is even worse when other phenomena, like fluid-particle heat transfer or particle collisions, are studied [1]. In fact, the long-standing experimental tools for investigating turbulent flows, such as hot-wire anemometry, at best only provide data on the velocity field and its spatial correlation function. Over the past few decades, new techniques have been developed, employing on fast-imaging to follow particles in turbulent flows. Such developments in experimental tools and methods have led to collecting a very new information about the motion of particles in turbulent flows, yet detecting collisions between a large number of tiny particles in a well-controlled laboratory experiment is not possible [2]. Therefore, direct numerical simulations (DNSs) have been always an important tool to obtain detailed results on features which cannot be directly measured. In fact, DNS provides a powerful tool to extend the existing insights into complex flow regimes like particle-laden turbulent flows, even if it is still limited to relatively low to medium Reynolds numbers due to the need for huge computational resources.

The interaction between fluid and particles in terms of thermal properties has been explored in several papers, mainly using the point-particle approach that applies to small sub-Kolmogorov particles. Most of the research has focused on channel flows [3–5] and homogeneous turbulence [6–8]. However, recently, a few studies have examined the fluid-particle thermal interaction in the time-evolving shearless thermal mixing layer generated at the interface between two fluid regions with different temperatures. This configuration can serve also as a benchmark for turbulence models. The studies investigated both one-way and two-way coupling regimes [9], with a focus on collisionless suspensions and the impact of particle inertia and Reynolds number.

Collisions between particles play a crucial role in heat transfer in fluidized beds because heavy particles are able to cross the wall thermal layer, thus transferring heat between the wall and the core region of the pipe. However, in such applications, volume fractions are high, usually on the order of 10^{-2} [10], well above the limit of two-way coupling between point particles. Only a few theoretical works have considered the effect of collisions on heat transfer, such as [11], who studied the heat transferred between elastically colliding spherical particles. Collisions are usually not taken into account when analyzing heat transfer by particles in a turbulent flow, despite their increased frequency with higher volume fractions. Carbone et al. [7] studied the effect of particle-particle collisions on temperature statistics in homogeneous and isotropic turbulence in the one-way coupling regime at low Reynolds numbers, finding a minor effect on small-scale temperature statistics. However, collisions can decelerate small particles while accelerating large ones, resulting in an enhanced velocity scattering that can affect particles' ability to carry enthalpy over long distances in the presence of a strong temperature gradient. This scattering impacts how the presence of particle particles can enhance heat transfer compared to an unseeded flow [9].

To investigate how inter-particle collisions impact heat transfer and fluid-particle correlations, we expanded on our previous research by examining the effect of elastic collisions in the simplest inhomogeneous flow configuration already considered in [9]. In this configuration, heat is transferred between two regions at different temperatures through a statistically steady homogeneous and isotropic velocity field, creating a mixing layer at the boundary between the two regions where fluctuations of temperature and velocities correlate. We compare single-point statistics with the collisionless regime in the same overall flow configuration [9]. In section 2, we provide a detailed description of the physical model and numerical methods used to simulate the collisional turbulent gas-particle flow. In section 3, we discuss the results from our simulations. A comparison between the Nusselt number variation in terms of Stokes number and Taylor micro-scale Reynolds number for collisional and collisionless flow regimes, as well as an analysis of the temperature of colliding particles is included. Finally, in section 4, we provide a brief summary of the main conclusions.

2. Physical model

2.1. Governing equations

In this study, we use an Eulerian-Lagrangian approach to model the dynamics of a non-homothermal incompressible flow seeded with particles. We distinguish between the continuous fluid phase and the discrete particle phase, with temperature variations assumed to be small enough to not significantly change fluid density. Therefore, within these hypotheses, the fluid phase is represented by the following system of equations:

$$\partial_i u_i = 0 \tag{1}$$

$$\partial_t u_i + u_j \partial_j u_i = -(1/\rho_0)\partial_i p + \nu \partial_j \partial_j u_i + f_{u,i}, \tag{2}$$

$$\partial_t T + u_j \partial_j T = \kappa \partial_j \partial_j T + (1/\rho_0 c_{p0})C_T. \tag{3}$$

where $\boldsymbol{u}(t,\boldsymbol{x})$, $T(t,\boldsymbol{x})$, and $p(t,\boldsymbol{x})$ are the fluid velocity, temperature, and pressure fields, respectively. The constants ρ_0, c_{p0}, ν, and κ represent the fluid density, isobaric specific heat capacity, kinematic viscosity, and thermal diffusivity, respectively. The body force $\boldsymbol{f}_u$ is introduced to maintain turbulent fluctuations in a statistically steady state, and C_T is the heat exchanged per unit time and unit mass with particles, representing the particle thermal back reaction on the flow. Similarly to previous works (e.g. [7–9]), we assume a one-way coupling regime for momentum exchange, so that no force is exerted by particles on the fluid. This assumption holds true in dilute regimes, as previous works have found that momentum feedback has a minor thermal effect on fluid temperature statistics [7].

Table 1: Dimensionless flow parameters.

Simulation		I	II	III
Taylor microscale Reynolds number	Re_λ	56	86	124
Taylor microscale	λ	0.226	0.29	0.35
Integral length scale	ℓ	0.40	0.74	0.94
Root mean square of velocity fluctuations	u'	0.59	0.71	0.85
Forced wavenumber	k_f	5	$\sqrt{6}$	$\sqrt{3}$
Prandtl number	Pr	0.71	0.71	0.71
mean turbulent kinetic energy dissipation rate	ε	0.25	0.25	0.25
Kolmogorov length scale	η	0.0153	0.0153	0.0153
Kolmogorov time scale	τ_η	0.098	0.098	0.098
Particle volume fraction	φ		4×10^{-4}	
Density ratio	ρ_p/ρ_0		10^3	
Stokes number ratio	$\mathrm{St}_\vartheta/\mathrm{St}$		4.43	
Stokes number	St		0.2 ; 0.3 ; 0.5 ; 0.7 ; 0.8 ; 0.9 ; 1 ; 1.2 ; 1.5 ; 2 ; 2.5 ; 3	

We consider the motion of a set of identical small, rigid spherical particles. The particles are assumed to have a radius R much smaller than the Kolmogorov length-scale η so that they are considered material points. They have a mass density much greater than the fluid density, making the Stokes drag force the dominant term in the Maxey-Riley equation [12]. An equation for the particle temperature can be derived under the same assumptions. Thus, the dynamics of each particle can be described by the following equations:

$$\frac{\mathrm{d}^2 x_{p,i}}{\mathrm{d}t^2} = \frac{\mathrm{d}v_{p,i}}{\mathrm{d}t} = \frac{u_i(t, \boldsymbol{x}_p) - v_{p,i}}{\tau_v}, \tag{4}$$

$$\frac{\mathrm{d}\vartheta_p}{\mathrm{d}t} = \frac{T(t, \boldsymbol{x}_p) - \vartheta_p}{\tau_\vartheta}, \tag{5}$$

where $\boldsymbol{x}_p(t)$, $\boldsymbol{v}_p(t)$, and $\vartheta_p(t)$ are the position, velocity, and temperature of the p-th particle, respectively. The momentum and thermal relaxation times τ_v and τ_ϑ are given by

$$\tau_v = \frac{2}{9}\frac{\rho_p}{\rho_0}\frac{R^2}{\nu}, \qquad \tau_\vartheta = \frac{1}{3}\frac{\rho_p c_{pp}}{\rho_0 c_{p0}}\frac{R^2}{\kappa}, \tag{6}$$

where ρ_p and c_{pp} denote the particle density and specific heat at constant pressure. Particle-particle interactions, other than collisions, are not considered. The particle thermal feedback per unit time and unit volume in equation (2) is given by

$$C_T(t, \boldsymbol{x}) = \frac{4}{3}\pi R^3 \rho_p c_{pp} \sum_{p=1}^{N_p} \frac{\mathrm{d}\vartheta_p(t)}{\mathrm{d}t}\delta(\boldsymbol{x} - \boldsymbol{x}_p). \tag{7}$$

where $\delta(\cdot)$ is the Dirac delta function.

2.2. Flow setup and numerical method

We investigate the heat transfer between two homogeneous regions with different temperatures, T_1 and $T_2 < T_1$, in a homogeneous and isotropic velocity field. To simulate this phenomenon, we solve the governing equations described in Section 2.1 in a parallelepiped domain with dimensions $L_1 = L_2$ and $L_3 = 2L_1$ along the x_1, x_2, and x_3 directions. The initial temperature distribution is set to T_1 in the half-domain where $x_3 < L_3/2$ and T_2 in the half-domain where $x_3 > L_3/2$.

We apply periodic boundary conditions to the velocity field on all faces of the domain, while for temperature, we decompose it into a mean linear field and a fluctuating part, as described in [9]. This allows us to apply periodic boundary conditions to the fluctuating part of the temperature field. Any particles that exit the domain are reintroduced on the opposite side.

The governing equations (1-7) are made dimensionless by using $L_1/2\pi$ as length scale, a velocity scale deduced from the imposed kinetic energy dissipation rate ε, and the temperature difference $T_1 - T_2$ as temperature scale [9]. To make the results more physically significant, the Taylor-microscale is used as the reference length in the definition of the Reynolds number. In the dimensionless form, the flow is governed by the Reynolds number $\mathrm{Re} = u'\lambda/\nu$, the Prandtl number $\mathrm{Pr} = \nu/\kappa$, and the particle-to-fluid heat capacity ratio $\varphi_\vartheta = \varphi(\rho_p c_{pp})/(\rho_0 c_{p0})$, where φ is the particle volume fraction. The particle dynamics are described by the Stokes numbers, which represent the ratio between their relaxation times and the flow timescales. To characterize the particle dynamics in terms of local fluctuations of fluid state, the Kolmogorov timescale $\tau_\eta = (\nu/\varepsilon)^{1/2}$ is used instead of the large-scale time used in the adimensionalization. Thus, the Stokes number $\mathrm{St} = \tau_v/\tau_\eta$ and the thermal Stokes number $\mathrm{St}_\vartheta = \tau_\vartheta/\tau_\eta$ are used to describe the particle dynamics. All relevant flow parameters are listed in table 1.

A fully dealiased pseudospectral method, using the 3/2-rule, was employed to discretize the spatial domain of the fluid phase equations (1–3). The forcing function f_u was defined in Fourier space as

$$\hat{f}_{u,i}(t, \boldsymbol{\kappa}) = \varepsilon \frac{\hat{u}_i(t, \boldsymbol{\kappa})}{\sum_{||\boldsymbol{\kappa}||=\kappa_f} ||\hat{u}_i(t, \boldsymbol{\kappa})||^2} \delta(||\boldsymbol{\kappa}|| - \kappa_f), \tag{8}$$

where ε denotes the energy injection rate, equal to the kinetic energy dissipation in statistically steady conditions, and κ_f is the forced wavenumber. Interpolation of fluid velocity and temperature at particle positions, and computation of the particle thermal feedback (7), were carried out using a recent numerical method [13, 14] based on inverse and forward non-uniform fast Fourier transforms with a fourth-order B-spline basis. Integration in time was performed for both the carrier flow equations (1–3) and the particle equations (4)–(5) using a second order exponential integrator.

2.3. Inter-particle collision model

In this study, we focus on elastic binary collisions that occur when the distance between the centres of two particles is equal to their diameter. To introduce these collisions into the numerical simulation, a first-order particle trajectory reconstruction is performed after each time step. Therefore, a collision between the p-th and q-th particles in a time step $t \in [t_n, t_{n+1})$ occurs when the following equation,

$$||(1 - \tilde{t})(\boldsymbol{x}_p(t_n) - (\boldsymbol{x}_q(t_n)) + \tilde{t}(\boldsymbol{x}p(tn + 1) - (\boldsymbol{x}_q(tn + 1))|| = 2r_p, \tag{9}$$

where $\tilde{t} = (t - t_n)/\Delta t$ has a real solution of (9) for $\tilde{t} \in [0, 1)$. In such a case, the positions and velocities of the colliding particles at the end of the time step are obtained from momentum and energy conservation, i.e. they move with the velocity achieved after the collision for the remaining part of the time step. It is assumed that no heat transfer occurs between colliding particles at the impact event and that no direct hydrodynamic interaction, except inter-particle collisions, is taken into account [15]. However, direct collision detection is computationally expensive and not feasible for a large number of particles N_p because it requires $O(N_p^2)$ numerical operations. To address this issue, the particles are grouped within small boxes, and particle collisions are only detected between particles within the same box. This approach is more practical and computationally efficient. The effect of the box boundaries can be eliminated by shifting the boxes and repeating the algorithm [15].

3. Results

This section provides a comparison between the heat transfer in the collisional and collisionless regimes, within the thermal two-way coupling regime with a constant thermal Stokes number to Stokes number ratio of 4.43, representative of water droplets in air. The visualization in Figure 1 shows the particles and their temperature as they move across the plane initially separating the two regions at different temperatures, being heated or cooled by the flow in the process. This flow configuration leads to a self-similar stage of evolution where all flow and particle statistics collapse when rescaled with the
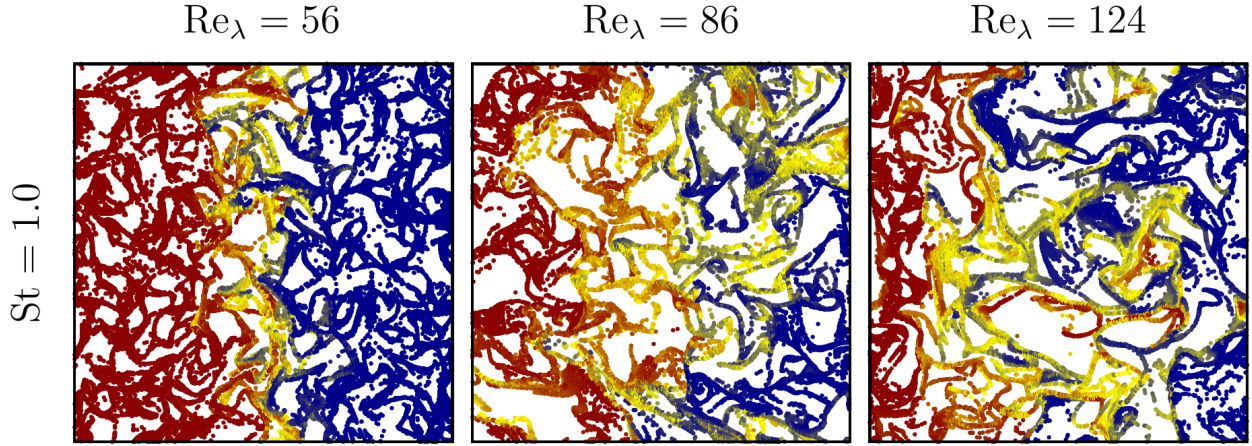
$$\text{Re}_\lambda = 56 \qquad \text{Re}_\lambda = 86 \qquad \text{Re}_\lambda = 124$$

St = 1.0

Figure 1: Visualization of particles with St = 1 in a small slab around a (x_1, x_3) plane after three eddy turnover times ℓ/u'. Particles, out of scale, are coloured according to their temperature, the red colour denotes the highest temperature in the domain, and the blue colour the lowest temperature.

mixing layer thickness δ. The mixing layer thickness can be defined as $(T_1 - T_2)/\max\{|\partial T/\partial x_3|\}$ [9, 16] and exhibits an almost diffusive time growth. This stage is reached after a few eddy turnover times $\tau = \ell/u'$, during which a high-temperature variance region develops in the thermally inhomogeneous region.

During this self-similar stage of evolution, the particle-to-fluid temperature variance ratio remains constant. It can be observed from Figure 2(a) that collisions tend to slightly reduce the variance of particle temperature compared to the fluid temperature, especially at larger Stokes numbers. Due to the particle thermal feedback, the fluid temperature variance increases more than the particle variance, particularly at large Stokes numbers, over the collisionless regime (see Figure 2(b)). However, this difference is small and could only become significant at higher volume fractions.

Figure 3 shows the most important result, that is the correlation between velocity and temperature fluctuations, which are proportional to the mean heat transfer across the layer separating the two homothermal regions. Indeed, the mean heat transfer in the inhomogeneous direction x_3 is given by

$$\dot{q} = -\lambda \frac{\partial \langle T \rangle}{\partial x_3} + \rho_0 c_{p0} \langle u_3' T' \rangle + \varphi \rho_p c_{pp} \langle v_3' \vartheta' \rangle \tag{10}$$

where the first term is the diffusive heat transfer, the second one is the carrier flow convection, and the last one is the particle contribution. By using standard dimensional analysis, it can be written in terms of the Nusselt number, defined as the heat flux normalized by the heat transfer in a static, non-moving system. In this flow, the mixing layer thickness δ is the only relevant length-scale, so that Nu $= \dot{q}/[\lambda(T_1 - T_2)/\delta]$. Dimensional analysis gives

$$\text{Nu} = \text{Nu}(\text{Re}_\lambda, \text{Pr}, \varphi_\vartheta, \text{St}, \text{St}_\vartheta)$$

where Re_λ is the Reynolds number, Pr is the fluid Prandtl number, $\varphi_\vartheta = \varphi(\rho_p c_{pp})/(\rho_0 c_{p0})$ is the particle-to-fluid heat capacity ratio, St and St_ϑ are the Stokes and thermal Stokes numbers, i.e. the rations between the particle momentum and thermal relaxation times and the Kolmogorov microscale, St $= \tau_v/\tau_\eta$, $\text{St}_\vartheta = \tau_\vartheta/\tau_\eta$. The Stokes and thermal Stokes numbers quantify particle inertia in dimensionless form. From (10), Nu can be decomposed in the flow and particle convection, i.e. Nu $= 1 + \text{Nu}_c + \text{Nu}_p$, where

$$\text{Nu}_c = \frac{-\langle u_3' T' \rangle}{\kappa |\partial \langle T \rangle/\partial x_3|}, \qquad \text{Nu}_p = \varphi_\vartheta \frac{-\langle v_3' \vartheta' \rangle}{\kappa |\partial \langle T \rangle/\partial x_3|} \tag{11}$$
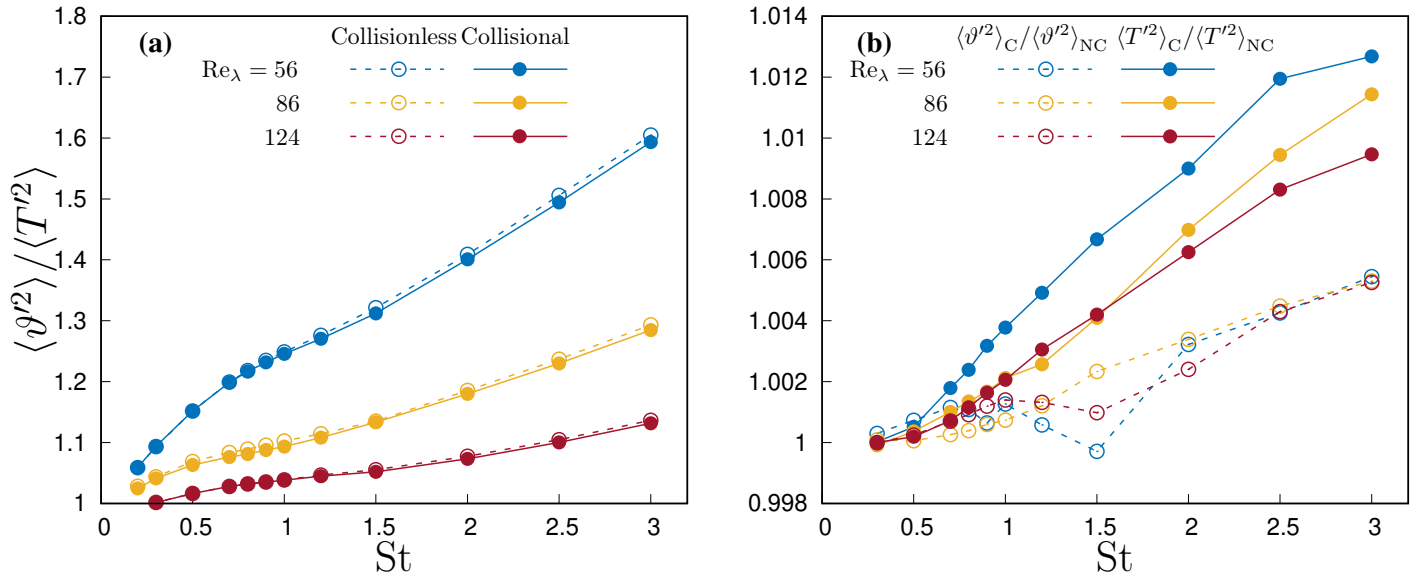
Figure 2: (a) Ratio between particle temperature variance and fluid temperature variance (b) particle-to-particle and fluid-to-fluid temperature variance ratio in two-way coupling simulations with and without collisions. Variances are measure in the central part of the domain, where heat transfer takes place.
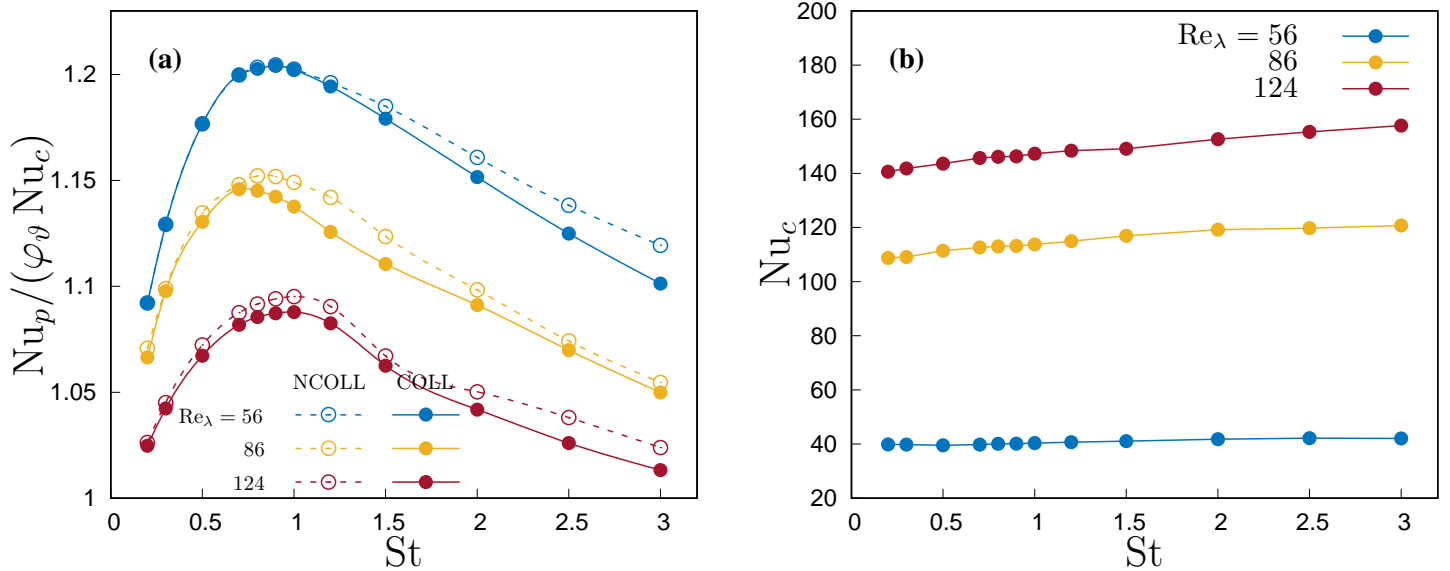

Figure 3: (a) Particle to fluid convective Nusselt number ratio as a function of the Stokes number at different Taylor microscale Reynolds numbers. (b) Convective Nusselt number as a function of the Stokes number. Solid lines indicate the collisional regime, while dashed lines denote collisionless simulations.
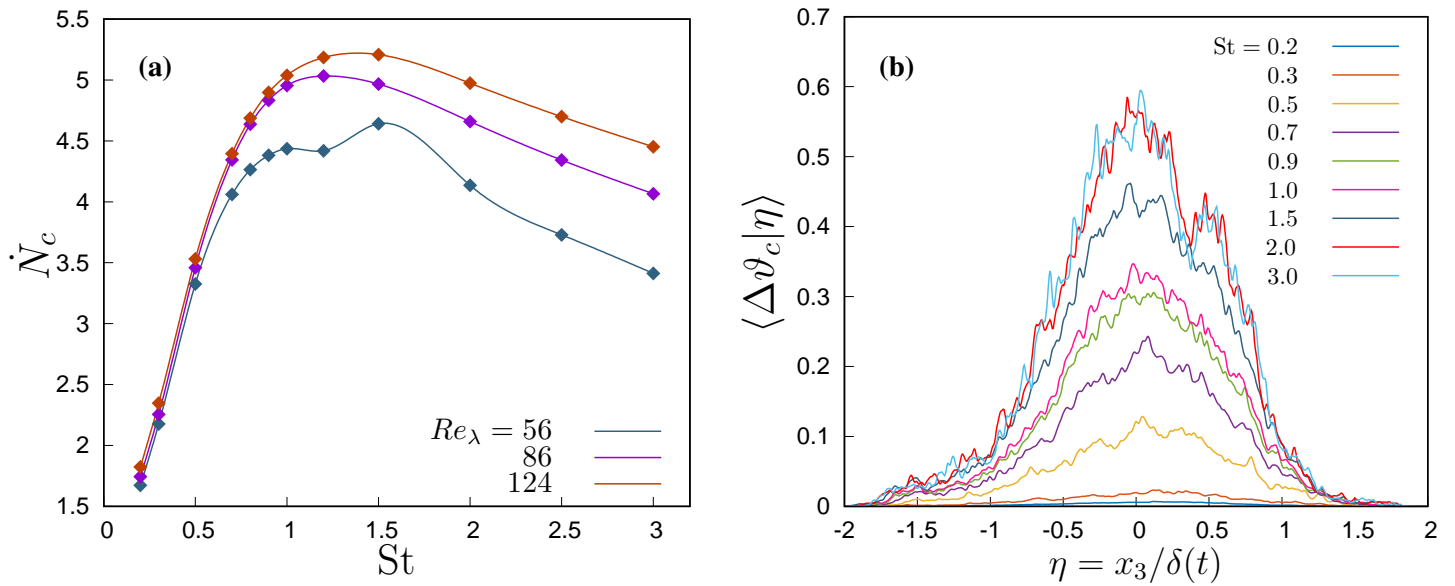
Figure 4: Mean collision rate, number of collisions per unit time and volume, and mean temperature difference between colliding particles pairs, $\Delta\vartheta_c = |\vartheta_a - \vartheta_b|$, where T_a and T_b are the temperatures of the colliding particles, conditioned by the normalized position η in the inhomogeneous direction.

The ratio $\mathrm{Nu}_p/\mathrm{Nu}_c$, equal to $\varphi_\vartheta\langle v_3'\vartheta'\rangle/\langle u_3'T'\rangle$, is the parameter which gives a measure of the contribution to the heat transfer through the non homothermal layer by the suspended particles. During the self-similar stage of the mixing layer the Nusselt number does not vary on time, because all fluxes are proportional since they scale with the same $\delta(t)$.

Figure 3(a) shows this ratio for three different Reynolds numbers as a function of the Stokes number. All quantities are computed in the centre of the domain, where correlations have their maxima. The ratio has a maximum when the Stokes number is of order one, that is, in correspondence of the highest particle clustering. In the vanishing inertia limit, i.e. when the Stokes number tends toward zero, particles move like passive tracers. However, since in our configuration also the thermal inertia tends to vanish in this limit, because $\mathrm{St}\_\vartheta/\mathrm{St}$ has been kept constant, thus we have $\mathrm{Nu}_p/(\varphi_\vartheta\mathrm{Nu}_c) \to 1$ when $\mathrm{St} \to 0^+$. On the opposite limit of very large inertia, when $\mathrm{St} \to \infty$, particles velocity and temperature tend to decorrelate from the fluid velocity and temperature, leading to a gradual reduction of $\mathrm{Nu}_p/(\varphi_\vartheta\mathrm{Nu}_c)$. The same trend can be observed at all the simulated Reynolds numbers. The influence of particles on the convective Nusselt number Nu_c is presented in figure 3(b). Particle inertia gradually modulates the Nusselt number, which increases with the Stokes number. However, collisions between particles do not produce any significant effect on the convection. This means that, at the volume fraction investigated, the deviation of particles from their trajectory induced by collision scattering has an overall minor impact on their mean thermal feedback on the fluid. On the contrary, collisions tend to attenuate the correlation between particle velocity and temperature and, consequently, the ability of particles to transport heat over long distances. The collision rate in an homogeneous turbulence is higher for larger particles, because their inertia decorrelate their velocity from the fluid velocity, and has a maximum when the Stokes number is of order one, approximately between 0.5 and 3, where the velocity decorrelation is coupled to clustering, as shown also in figure 4(a), so that the impact of collisions is more evident at larger St. We could attribute the reduction of the temperature-velocity correlation we observed to the fact that collisions between particles with very different temperatures occur between particles coming from distant zones in the inhomogeneous direction, which is possible only for large inertia and thermal inertia, but collisions generates a scatter that modifies their velocity in the x_3 direction, not their temperature, thus reducing the $\langle v'\vartheta'\rangle$ correlation. Indeed, the temperature difference between colliding particles increases with the Stokes number, see figure 4(b), an indication that higher particle inertia allows for collisions between particles coming from very distant regions, allowing them to cross temperature fronts [7], while their thermal inertia allows them to keep their temperature.

4. Conclusion

In this study, we investigated the impact of particle collisions on heat transfer in a particle-laden turbulent flow, where the volume fraction of particles was fixed at $\varphi = 4 \times 10^{-4}$ and the regime was dilute, allowing for a point-particle approach. We have shown that particle collisions have a minimal effect on heat transfer when the Stokes number was less than 1, but, when the Stokes number is larger than 1, there is a slight reduction, of about 10%, in the particle-velocity-temperature correlation. Nevertheless, we can conclude that collisions do not significantly affect the ability of particles to modulate fluid temperature fluctuations. Based on these results, we infer that incorporating collisions into bulk models of heat transfer in dilute particle-laden flows is unnecessary.

Acknowledgements

References

[1] A. Pumir and M. Wilkinson, "Collisional aggregation due to turbulence," *Annual Review of Condensed Matter Physics*, vol. 7, no. 1, pp. 141–170, 2016.

[2] F. Toschi and E. Bodenschatz, "Lagrangian properties of particles in turbulence," *Annual Review of Fluid Mechanics*, vol. 41, no. 1, pp. 375–404, 2009.

[3] F. Zonta, C. Marchioli, and A. Soldati, "Direct numerical simulation of turbulent heat transfer modulation in micro-dispersed channel flow," *Acta Mechanica*, vol. 195, pp. 305–326, 2008.

[4] J. G. M. Kuerten, C. W. M. van der Geld, and B. J. Geurts, "Turbulence modification and heat transfer enhancement by inertial particles in turbulent channel flow," *Phys. Fluids*, vol. 23, no. 12, pp. 123301/1–8, 2011.

[5] F. Rousta and B. Lessani, "Near-wall heat transfer of solid particles in particle-laden turbulent flows," *International Communications in Heat and Mass Transfer*, vol. 112, pp. 104475/1–7, 2020.

[6] J. Béc, H. Homann, and G. Krstulovic, "Clustering, fronts, and heat transfer in turbulent suspensions of heavy particles," *Physical Review Letters*, vol. 112, pp. 234503/1–5, 2014.

[7] M. Carbone, A. D. Bragg, and M. Iovieno, "Multiscale fluid–particle thermal interaction in isotropic turbulence," *J. Fluid Mech.*, vol. 881, pp. 679–721, 2019.

[8] I. Saito, T. Watanabe, and T. Gotoh, "Modulation of fluid temperature fluctuations by particles in turbulence," *J. Fluid Mech.*, vol. 931, p. A6, 2022.

[9] H. R. Zandi Pour and M. Iovieno, "Heat transfer in a non-isothermal collisionless turbulent particle-laden flow," *Fluids*, vol. 7, no. 11, pp. 345/1–24, 2022.

[10] F. Jiang, H. Wang, Y. Liu, G. Qi, A. E. Al-Rawni, P. Nkomazana, and X. Li, "Effect of particle collision behavior on heat transfer performance in a down-flow circulating fluidized bed evaporator," *Powder Technology*, vol. 381, pp. 55–67, 2021.

[11] J. Sun and M. M. Chen, "A theoretical analysis of heat transfer due to particle impact," *Int. J. Heat Mass Transfer*, vol. 31, pp. 969–975, 1988.

[12] M. R. Maxey and J. J. Riley, "Equation of motion for a small rigid sphere in a nonuniform flow," *Phys. Fluids*, vol. 26, no. 4, pp. 883–889, 1983.

[13] M. Carbone and M. Iovieno, "Application of the non-uniform fast fourier transform to the direct numerical simulation of two-way coupled turbulent flows," *WIT Trans. Eng. Sci.*, vol. 120, pp. 237–248, 2018.

[14] M. Carbone and M. Iovieno, "Accurate direct numerical simulation of two-way coupled particle-laden flows through the nonuniform fast fourier transform," *Int. J. Safety and Sec. Eng.*, vol. 10, no. 2, pp. 191–200, 2020.

[15] R. Onishi, K. Takahashi, and J. C. Vassilicos, "An efficient parallel simulation of interacting inertial particles in homogeneous isotropic turbulence," *Journal of Computational Physics*, vol. 242, pp. 809–827, 2013.

[16] H. R. Zandi Pour and M. Iovieno, "The effect of particle collisions on heat transfer in a non-isothermal dilute turbulent gas-particle flow," *8th World Congress on Momentum, Heat and Mass Transfer*, 03 2023.